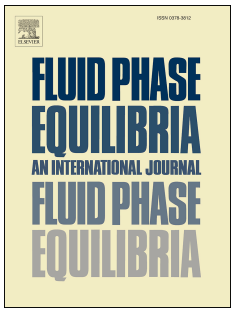

Lattice-gas Monte Carlo study of sI clathrate hydrates of ethylene: Stability analysis and cell distortion

Pablo Longone, Ángel Martín, Antonio J. Ramirez-Pastor

PII: S0378-3812(20)30286-7

DOI: https://doi.org/10.1016/j.fluid.2020.112739

Reference: FLUID 112739

To appear in: *Fluid Phase Equilibria*

Received Date: 13 December 2019

Revised Date: 29 May 2020

Accepted Date: 23 June 2020

Please cite this article as: P. Longone, Á. Martín, A.J. Ramirez-Pastor, Lattice-gas Monte Carlo study of sI clathrate hydrates of ethylene: Stability analysis and cell distortion, *Fluid Phase Equilibria* (2020), doi: https://doi.org/10.1016/j.fluid.2020.112739.

Credit author statement

Pablo Longone: Conceptualization, Methodology, Software, Writing-Original draft preparation.

Ángel Martín: Conceptualization, Writing- Reviewing and Editing,

Antonio J. Ramirez-Pastor: Conceptualization, Methodology, Writing-Original draft preparation

Lattice-Gas Monte Carlo Study of sI Clathrate Hydrates of Ethylene: Stability Analysis and Cell Distortion

Pablo Longone[a,*], Ángel Martín[b] and Antonio J. Ramirez-Pastor[a]

[a]*Departamento de Física, Instituto de Física Aplicada (INFAP), Universidad Nacional de San Luis, CONICET, Ejército de los Andes 950, D5700HHW San Luis, Argentina.*

[b]*Departamento de Ingeniería Química y Tecnología del Medio Ambiente, Facultad de Ciencias, Universidad de Valladolid, 47011 Valladolid, Spain.*

Abstract

In this paper, a two-dimensional lattice-gas model is applied to study the stability and lattice distortion of sI clathrate hydrates of ethylene. Two levels of approximation are considered for the lateral interactions between the adsorbed molecules. By using Monte Carlo simulations, adsorption isotherm (coverage of the cavities as a function of the chemical potential), degree of deformation of the sI structure, and free energy of the adsorbed phase are obtained. A direct relationship between cell distortion and cell occupancy is observed. In addition, the minimum distortion coincides with the minimum value of the free energy. Accordingly, the stability phase diagram can be calculated from the values of the chemical potential at the minimum deformation. The obtained results indicate that the most stable condition of the system occurs for values of the cavity density ranging between 0.35 and 0.4. Finally, MC results are compared with data from experiments and more complex simulations.

Keywords:
Clathrate hydrates
Lattice-gas model
Monte Carlo simulations
Ethylene

1. Introduction

Clathrate hydrates are a certain kind of inclusion compounds formed by a mixture of water and components of low molecular weight [1, 2]. Through hydrogen-bonds, water molecules form a regular crystalline lattice containing cavities that are occupied by molecules from a guest gas. The partial adsorption of the guest molecules within their cavities gives stability to the system, hence, forming clathrate hydrates of gases. The cavities show different shapes and sizes; pentagonal dodecahedron (5^{12}), tetrakaidecahedron ($5^{12}6^2$),

hexakaidecahedron ($5^{12}6^4$), irregular dodeca-hedron ($4^35^66^3$), and icosahedrons ($5^{12}6^8$). The symbols between parenthesis correspond to Jeffrey`s Notation of Cavities [3, 4]. The combination between different numbers and types of cavities builds up unit cells which form hydrate structures such as sI, sII and sH [1, 2]. Hydrate structures sI and sII are those most frequently observed, which consist on ($5^{12}6^2$) and ($5^{12}6^4$) groups, 12 pentagonal with 2 hexagonal water molecule rings (24 water molecules) and 12 pentagonal with 4 hexagonal water molecule rings (28 water molecules), respectively. Both structure and stability of the regular crystalline lattice depend on the nature, size and shape of the guest molecules that occupy the cavities. Gas molecules such as methane, ethylene, ethane as well as carbon dioxide form type sI hydrates. Large molecules, on the other hand, would rather form II structure (propane, iso-butane) and sH (cyclohexane, cycloheptane).

Over the last 100 years, large quantities of methane have been found in deposits of hydrate located in natural geological environments such as in the depths of the ocean as well as in the permafrost deposits in the arctic region. These large quantities of methane have come to represent a new and powerful source of energy for the future [5–7]. It has been estimated that there are more energy resources in these hydrates than in conventional fossil fuels [8, 9]. Furthermore, during natural gas extraction, clathrate hydrates block the pipelines, under conditions of low temperature and high pressure, which is highly relevant at industrial level [10]. On another note, attention has been drawn to the use of hydrates as a mean of energy and mass storing [11, 12]. Recent attempts have been laid on separation technology based on clathrate hydrates, which mainly consists on the selective partition of the components in both the hydrate phase and the gas phase [13-17]. The growing interest in the Greenhouse Effect has also produced an increase in the interest on the capture of $CO_2$for the formation of hydrates [14-18].A further attractive example of technology that is based on hydrate separation is the process of concentration of aqueous solutions [19-22], such as in desalination and juice concentration. S. Li et al. [23] used clathrate hydrates of ethylene to simplify the concentration of orange juice. An adsorption–hydratation hybrid method was used for the separation of hydrocarbons [24, 25, 26] such as the mixture of gases C_2H_4 / CH_4.

Ethylene is one of the most important gases in the industrial level; it is also a special gas due to its great molecular size which within a wider range of temperature [27] forms

hydrates that have a potential application either in storage or separation. These investigations, carried out basically focused on the conditions of formation and occupation of cavities of ethylene hydrates [27, 28, 29, 30], have become highly important. Likewise, the separation of ethylene from the mixture of gases [27, 30-35], have become fundamental. In these research papers, it is suggested that the formation pressure of ethylene hydrates to the same temperature is considerably lower than CH_4, C_2H_6, CO_2, etc. [1, 27–36].

In order to be able to theoretically predict the conditions of formation and occupation (quantity of gas storage) of clathrate hydrates, different accurate thermodynamic models have been developed. The theory of Van der Waals and Platteeuw (vdWP) [37] was developed in 1958, combining statistical mechanics with the classical theory of adsorption (Langmuir model). In this theory, it is supposed that interactions between guest molecules and aqueous lattice are relatively weak and are limited to the gas molecule nearest neighbors (NN). Besides, the interactions between the guest molecules from the neighboring cavities are neglected, consequently, only the simple occupation of guest gas molecules is considered. Hence, the behavior of each guest molecule does not depend on the presence of other guest molecule. Some modifications were late introduced to this model, like multiple occupancy and flexibility of cavities [38-41]. Nevertheless, the theory of vdWP is currently the most important and widely used theoretical tool in the study of gas hydrate.

Along the last years, computer simulations have proved to be a useful tool for studying occupation and stability of clathrate hydrates [42-50]. By doing a comparison between experiments and theoretical models, the importance of numerical simulations [49, 50] has been tested. By using Monte Carlo (MC) simulations, Pimpalgaonkar et al. could determine the triple point lines for methane hydrates and ethane [49]. Papadimitriou et al. reported the number of occupied cavities for He and THF mixed hydrates [50]. Results showed that large cavities were completely occupied by THF molecules, whereas the small cavities were partially occupied by He atoms.

It is widely known that there are effects of lattice distortion in the clathrate hydrates when the cavities are occupied by guest species of different sizes. Zele et al. [44] show through a study of molecular dynamic (MD) how the volume of the cell increases according to the different sizes of the guest species, which produces a distortion in the chemical potential.

This expansion in the lattice causes an increase in the difference within the chemical potential of water in empty and filled lattice. Martín and Peters [51] carried out a modification to the theoretical model vdWP [37] introducing a distortion model of chemical potential in order to model lattice distortion. The larger the size of the guest species, the higher is the importance of the distortion in the chemical potential. Sizov and Piotrovskaya [46] studied the behavior of methane clathrate hydrates for flexible and rigid lattice. Through MC simulation in the grand canonical ensemble (a three dimensional algorithm), isotherms of occupancy and phase diagrams were determined for the flexible and rigid hydrates. These results qualitatively agreed with the experimentations. Simulations were carried out using the model SPC / E for water [52] and the model UA was used for methane molecules [53]. The system used contained eight (2x2x 2) methane hydrate unit cells with 3D periodic boundary conditions. In 2015, we developed a 2D lattice-gas model and MC simulations for the study of the stability and distortion of sI structure in methane and carbon dioxide clathrate hydrates [54]. This was the first study of clathrate hydrates using a 2D lattice gas model with a reduced number of parameters compared to the works previously mentioned [42-50]. The data allowed us to make phase diagrams that qualitatively agree with theoretical as well as experimental predictions from the literature. We finally concluded that the minimum degree of deformation coincides with one molecule per cavity as well as with the minimum range of free energy. Furthermore our 2D lattice gas model captures the essence of the phenomena of distortion and stability in clathrate hydrates occupied by the guest molecules.

The main objective of this paper is to extend our previous model to study the degree of deformation of sI gas hydrates in the presence of ethylene, predicting the conditions in which hydrate is more stable through the degree of deformation. The present study is a natural continuation of our previous work and complements the results obtained in P. Longone et al. [54].

The rest of the paper is organized in the following way. The details of the model and MC simulation scheme are given in Section 2. The results are presented and discussed inSection3. Finally, the conclusions are drawn in Section 4.

2. Lattice-gas model and Monte Carlo simulation scheme

2.1 Lattice-gas model: sI hydrate structure

In this stage, we modeled, using a 2D discrete lattice-gas model and MC simulations, the distortion of the sI structure in the presence of the guest specie ethylene. The structure is reduced from 3D to 2D which then behaves as a discrete surface of adsorption sites wiFth a triangular geometry. Each lattice site, which is a part of the sI structure, represents an active adsorption center. The guest molecule adsorbs on the surface occupying more than one site (multisite occupancy must be considered). The hydrate is assumed to be stable previous to doing the simulations [42-50].

We consider a portion of sI clathrate hydrates composed by eight (2x2x2) unit cells, see Fig.1a. [55].Each unit cell contains two dodecahedron cavities (5^{12}) (small cavity) and six tetrakaidecahedron cavities ($5^{12}6^2$) (large cavity). The 3D points in blue correspond to water molecules.

Fig. 1b.corresponds to a face of the structure observed in Fig. 1a. along the direction of x, y or z axes. If we make a transversal cut parallel to xz plane we obtain Fig. 1b. , then if we cross through the center of the structure (8 unitary cells) with dotted line 2, we can observe that the sI structure is divided in two symmetrical parts. These two parts have their equivalent face to those faces on the extremes indicated by lines 1 and 3. Since faces 1, 2 and 3 are equivalent, we concluded on the feasibility of studying the behavior of the hydrates when the guest species try to occupy the cavities producing then a deformation on a 2D plane. This allows us to make an analogy between the adsorption-diffusion models and the multisite-occupancy adsorption model [56-58].

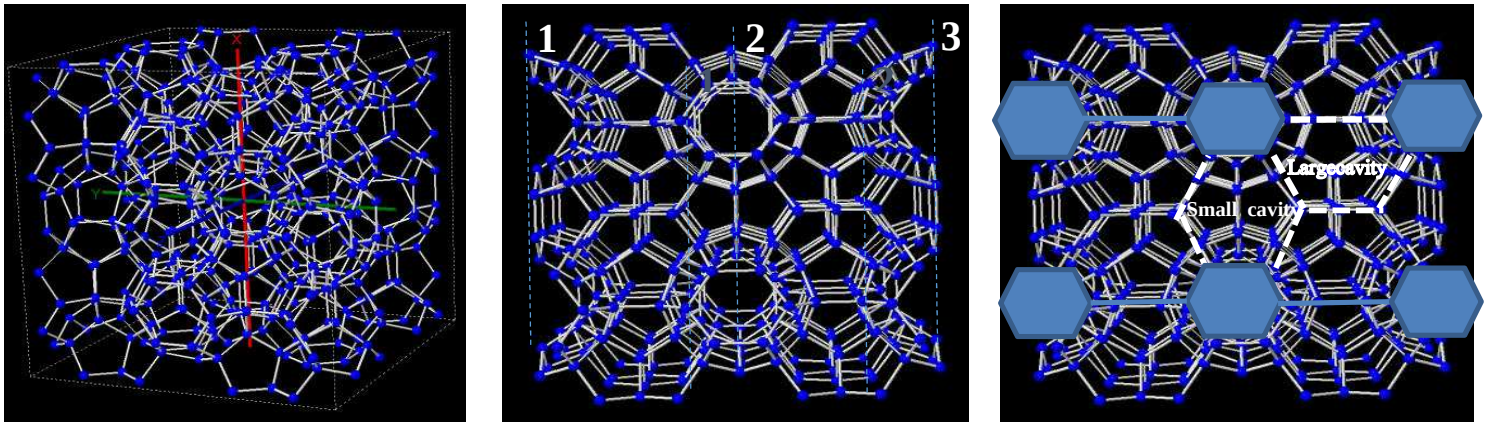

a) **b)** **c)**

Figure 1: (a) Three-dimensional scheme of a portion of sI clathrate hydrate composed by eight (2x2x2) unit cells. (b) Part (b) is a view observing the structure of part (a) in one direction along either the x, y or z axis. (c) Identification of water molecules that form the hexagons which build up the structure sI in 2D.

In Fig. 1c. , it can be observed both, the presence of hexagons formed by the water molecules, as well as the empty spaces that correspond to large and small cavities (represented by dotted lines). These hexagons form parallel chains separated by empty spaces that correspond to cavities over the plane. The structure shown in Fig. 1c. can be mapped to a discrete triangular lattice (Fig. 2). The water molecules will be the sites occupied by the monomers (which occupy a single site) forming hexagons that correspond to the superior part of the cavity, while the empty spaces correspond to the small and large cavities. The triangular lattice has high connectivity (c=6) which allows us to build a structure formed by parallel chains of spaced hexagons within a distance that represents the cavities of sI hydrate in 2D as it had been previously observed in 3D. In Fig. 2, we can observe that the small cavities are formed by three empty sites while large cavities are formed by 5. Finally, in Fig. 2, sites O do not represent water molecules however they are able to move to close neighbors. The reason why there are sites O is due to the fact that the water molecule crosses underneath this site being closed to the plane where the transversal cut was done Fig. 1b. Any guest molecule near site O does not energetically interact. Nonetheless, the site O is able to move because of the strain produced by the guest molecule.

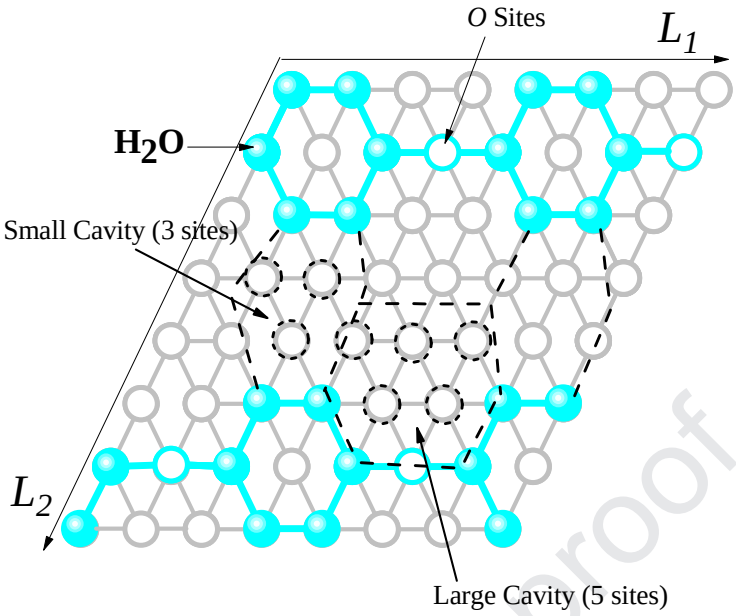

Figure 2: 2D lattice-gas model for the structure sI of clathrate hydrates. Water molecules are represented by previously adsorbed monomers on single sites. Empty sites between the chains of hexagons form the cavities.

2.2 Lattice-Gas Model: Host Species or Adsorbates

Host species are modeled by multisite occupancy in an adsorption model [56-58]. In this scheme, each ethylene guest molecule is considered an adsorbate molecule which has six units and each one of them occupies one single site in the lattice. The ethylene molecule cannot rotate on the axis of the carbon-carbon double bond. All the atoms are on the same plane [59] which is represented by the occupancy of six sites in the lattice (Fig. 3a.). In the simulation process the adsorption of an ethylene molecule is carried out as follows: once the first monomer, representing the carbon atom, is in this place, the second monomer (second carbon atom) occupies one of the three nearest neighbors to the first monomer since there are three possible directions. As soon as the second neighbor is occupied, the direction, the geometry and the remaining neighbors (hydrogen atoms) of the ethylene molecule (see Fig.3a.) are defined.

In order to have a better understanding of the adsorption process, we introduced the methane molecule as a referent through a 2D lattice-gas model, which had been previously studied [54] (see Fig. 3b.). The most stable occupation for methane hydrate can be observed in the following Fig. 3b. The methane molecule has tetrahedral symmetry with three

vertices in its base; accordingly, it is represented by the occupancy of three sites (forming a triangle) in the lattice. Thus, while the CH_4 molecule occupies only two sites of length along the three directions (Fig. 3b.), the C_2H_4 molecule extends over three length constants along the three directions in the lattice (Fig. 3a.). These size differences (the ethylene molecule being larger than the methane molecule) have been already observed in terms of Van der Waals diameters [60], Lennard-Jones size term [61-64], etc. It is important to highlight that the geometry over the plane of the adsorbates plays a key role in our model due to the fact that the molecules show geometries in accordance to the real ones. The C_2H_4 shows the two carbon atoms linked along a possible direction, the positions in the diagonal to this direction define the occupation of the hydrogen atoms in the lattice.

In order to describe the lateral interactions between the*m* and *n* species (*m*, *n*∈ C_2H_4, H_2O),the standard Lorentz-Berthelot of mixing rules has been used [51, 54, 65-67]

$$w_{m,n} = \frac{l_{m,n}\sqrt{\varepsilon_m \varepsilon_n}}{k}, \quad (1)$$

where $l_{m,n}$ is an interaction parameter that can be correlated to experimental cage occupancy data. As in Refs. [51, 54], it has been assumed that $l_{m,n}$ = 1. ε_m (ε_n) represents the characteristic energy corresponding to the *m* (*n*) species. In this paper, ε_m/k_B = 328.2 K (C_2H_4) and ε_n/k_B = 102.134 K (H_2O), where k_B is the Boltzmann constant (see Ref. [51] for a more detailed discussion about ε_m and ε_n). Given that $w_{m,n}$ represents the site-site lateral interaction, a factor *k* is used in the denominator due to the number of units in the molecule: *k*=6 for C_2H_4-C_2H_4 and H_2O-C_2H_4 interactions, and *k*=1 for H_2O-H_2O interactions.

Two levels of approximation are considered for the lateral interactions between the adsorbed molecules. For the first degree of approximation (scheme 1), it is assumed that an ethylene molecule interacts with the surrounding species through its four ends (see Fig. 3a.). For the second degree of approximation (scheme 2), the interactions corresponding to the internal units of the ethylene molecule are considered (see Fig. 3b.). Accordingly, scheme 1(2) accounts for 20(26) couplings for one ethylene molecule completely surrounded by occupied sites.

In both approximations, the magnitude of the lateral interaction between adsorbed units is homogeneous and equal to $w_{m,n}$. A more detailed description, distinguishing the couplings between the different units forming the ethylene molecule will be object of future research.

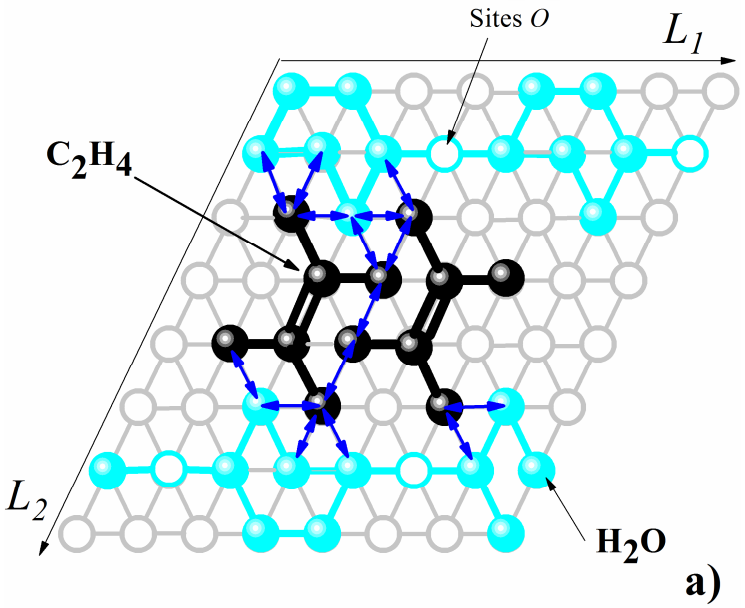

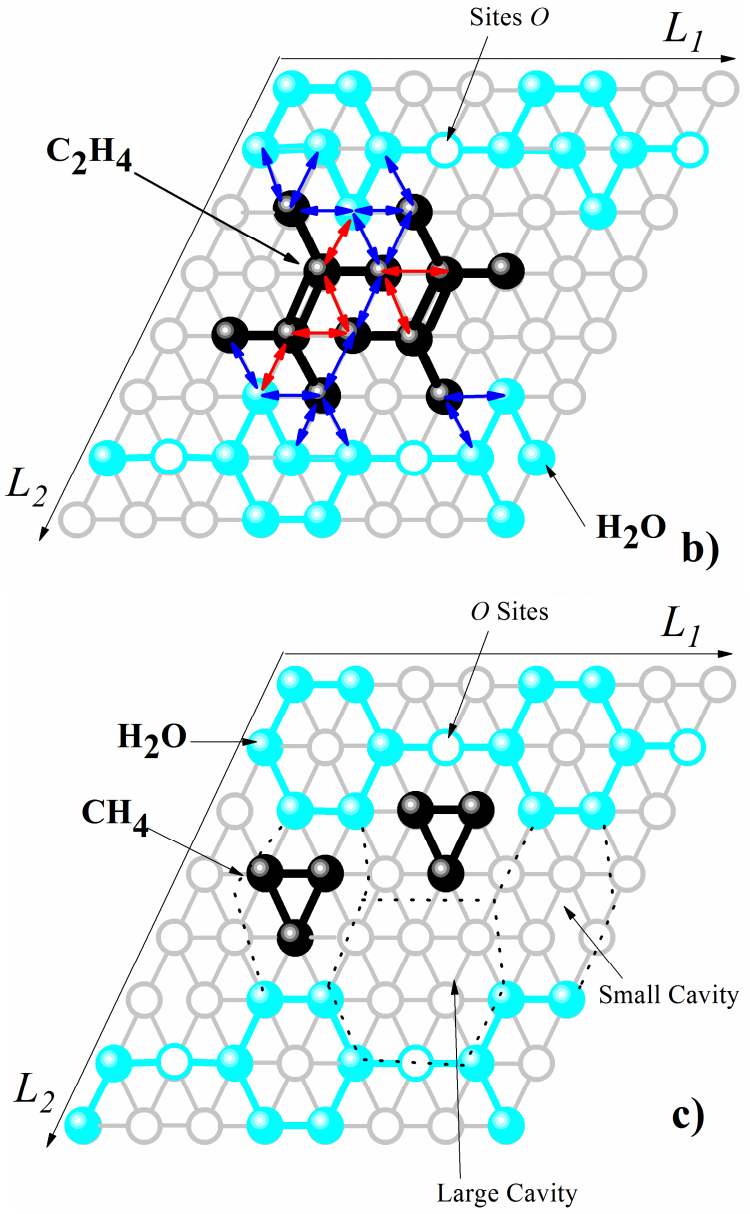

Figure 3: (a) Guest ethylene species adsorbed on large cavities. Guest molecules of ethylene deform the cavity when they are adsorbed. The figure shows two ethylene molecules interacting according scheme 1. Lateral interactions between nearest-neighbor adsorbed units are denoted by double-headed arrows. (b) Same as part (a) for two ethylene molecules interacting according scheme 2. (c) Guest methane species adsorbed on large and small cavities.

2.3 Monte Carlo Simulation Scheme and Thermodynamic Quantities

As described in Section 2.1, sI hydrate structure is represented by a 2D triangular lattice (along with an hexagonal lattice), where the monomers previously adsorbed represent the water molecules forming chains of hexagons, while the empty sites determine the large and small cavities. The adsorbate molecules (C_2H_4) are modeled as six adsorption units (each one occupying a lattice site) having diverse shapes along the three directions of the triangular lattice. The surface of the hydrate is represented by a matrix of $M=L_1xL_2$ adsorption sites with periodical boundary conditions. Nonetheless, the number of active adsorption sites is $M^*=L_1xL_2-(N_{H2O} + N_O)$, where N_{H2O} (N_O) is the number of H_2O molecules (*O* sites) in the sI structure.

In order to describe a system consisting of *N* adsorbed molecules on *M** sites at a given temperature *T*, the occupation variable c_i is introduced: c_i=0 if the site *i* is empty, and c_i=1 if the site *i* is occupied. On the order hand, guest molecules are adsorbed or desorbed as a unit, neglecting any possible dissociation. Under these considerations the energy of the system is given by;

$$E = \sum_{\langle i,j \rangle} \left[w_{11}\delta_{c_i,1}\delta_{c_j,1} + w_{22}\delta_{c_i,2}\delta_{c_j,2} + w_{1,2}\left(\delta_{c_i,1}\delta_{c_j,2} + \delta_{c_i,2}\delta_{c_j,1}\right)\right] - kN w_{11} \quad (2)$$

where δ is the Kronecker delta function; w_{11} obtained fromeq1 and represents the NN interaction between guest molecules(C_2H_4–C_2H_4); w_{22}eq.(1) is the NN interaction between water molecules (H_2O–H_2O); and w_{12} eq.(1) corresponds to the NN interaction between a guest molecule and a water molecule (C_2H_4–H_2O). w_{11} w_{12} and w_{22} are considered attractive interactions (w_{11}, w_{12}, w_{22}<0). <*i*,*j*> represents all pairs of NN sites. The term kNw_{11} is subtracted in eq.(2) since the summation over all the pairs of NN sites overestimate the total energy by including kNw_{11} internal bonds belonging to the *N* adsorbed guest molecules. As it can be seen from Fig. 3a. , *k* = 6 for C_2H_4 molecules.

The process is simulated through MC simulations in the grand canonical ensemble, using a typical adsorption–desorption algorithm [56-58]. The algorithm consists in carrying out a number of Monte Carlo stages (MCS) with the aim of equilibrating the system. After that, a new set of MCS evaluation is done. Thermodynamic quantities of interest (such us a deformation degree or coverage degree) are obtained in order to reach an average value. Typically, the equilibrium state can be appropriately reproduced after discarding the first $r=10^7$ MCs. In that case the next $r=2x10^7$ MCs are used to calculate averages. This is

performed for fixed values of temperature T and chemical potential μ (or fugacity in an alternative formulation). An elementary MCS can be detailed as follows:

1. Set the values of chemical potential μ and temperature T.

2. Choose randomly one of the M sites, and generate a random number $\xi \in [0, 1]$.

2a. If the selected site is empty, an attempt is made to adsorb a guest molecule as described in Section 2.2. The molecule is adsorbed if $\xi < W$, being W the Metropolis probability, $W=\min\{1,\exp[-\beta(\Delta E-\mu\Delta N)]\}$ with $\Delta N = +1$ [68]. $\beta=1/k_BT$ and $\Delta E = E_f - E_i$ is the difference between the energies of the final and initial states.

2b. If the selected site is occupied with a guest molecule, an attempt is made to desorb the molecule as described in Section 2.2. The molecule is desorbed if $\xi < W$, being W the Metropolis probability with $\Delta N = -1$.

2c. If the selected site is occupied with a H_2O molecule that has not been previously displaced, one of its six NN sites is randomly chosen. If the site is empty, an attempt is made to move the molecule toward the selected site. The molecule is moved if $\xi < W$, being W the Metropolis probability with $\Delta N = 0$.

2d. If the selected site is occupied with a H_2O molecule that has previously been displaced from its initial position, an attempt is made to return the molecule to the initial configuration. The molecule is moved if $\xi < W$, being W the Metropolis probability with $\Delta N = 0$.

3. Repeat from step (2) M times.

In the MC simulations, we varied the chemical potential μ, monitoring the simple density θ, and the density of cavities θ_{cavity}

$$\theta = \frac{6\langle N \rangle}{M*} \text{ and } \theta_{cavity} = \frac{\langle N \rangle}{\text{number of cavities}}, \quad (3)$$

where $\langle \ldots \rangle$ means the average over the MC simulation runs. Once $\mu(\theta)$ is obtained, the free energy per site is calculated by using the thermodynamic integration method [69]. The method in the grand canonical ensemble relies on the integration of the chemical potential μ coverage along a reversible path between an arbitrary reference state and the desired state of the system. Thus, for N particles on M^* lattice sites,

$$F\left(N, M^*, T\right) = F\left(N_0, M^*, T\right) + \int_{N_0}^{N} \mu dN' . \quad (4)$$

In our case, the determination of the free energy in the reference state, $F(N_0,M^*,T)$, is trivial [$F(N_0,M^*,T) = 0$ for $N_0 = 0$]. Note that the reference state, $N \rightarrow 0$, is obtained for $\mu/k_BT \rightarrow -\infty$. Finally, eq. (4) can be written in terms of intensive variables,

$$f = \int_0^{\theta} \frac{\mu(\theta')}{6} d\theta' \quad (5)$$

Finally we define the degree of deformation D of the lattice as,

$$D = \frac{\langle N_{mov} \rangle}{N_{H_2O} + N_O}, \quad (6)$$

where N_{mov} is the number of H_2O molecules and O sites that move from their original locations; and $N_{H2O}+ N_O$ is the total number of H_2O molecules and O sites forming the sI structure without deformation.

3. Results and discussion

The adsorption of ethylene guest molecules (each one occupying six sites on a triangular lattice representing the sI clathrate hydrate structure) was studied using a 2D lattice-gas MC simulation scheme. The water molecules are represented by monomers previously adsorbed forming chains of hexagons along the lattice (see Fig. 2). These monomers can move to neighboring sites and return from an equivalent distance to the lattice constant. A simple finite-size analysis was carried out by using lattices with different sizes. With $M=L_1 \times L_2 = 80 \times 128$ (3072 H_2O molecules and 512 O sites), we verified that finite-size effects are negligible. Then, the chemical potential μ was used as control parameter and the values of θ_{cavity} were calculated as simple averages. The occupation of the ethylene molecules in clathrate hydrates still remains a work in progress.

Ethylene is characterized for having a geometry and size which would prevent the occupation of smallest cavities. Thus, ethylene molecules would only occupy the largest cavities over the sI structure making the hydrate stable [70]. Nevertheless, some authors state that the ethylene guest molecules could eventually occupy the small cavities in the sI structure [30]. It is through the detection of two peaks in Raman crystal dispersion of ethylene hydrate that the presence of ethylene molecules in small cavities becomes evident. In our 2D lattice-gas model, there is one small cavity every two large ones. This means that approximately 2/3 of empty sites correspond to large cavities while the 1/3 remaining corresponds to small cavities.

Fig. 4 shows the adsorption isotherms (θ_{cavity} as a function of the chemical potential μ) for ethylene (circles) and methane (squares) at T = 275 K. Lateral interactions were included according to scheme 1 (see Section 2.2). In the case of ethylene, the saturation point is reached when the occupancy of the cavities is θ_{cavity} = 2/3. At these conditions, the guest molecules occupy the largest cavities, generating a distortion in the lattice and preventing the occupancy of the small cavities. In fact, the geometry and size of the ethylene molecule deforms the occupied cavities, increasing its size. This increase in the size of the largest cavities is at the expense of a corresponding decrease in the small cavities. The resulting size of the small cavities does not allow the adsorption of ethylene molecules. Nevertheless, as it is shown in Fig. 2a. , the small cavities can be occupied at low coverage, producing a great distortion as well as instability in the lattice. This point will be discussed in detail in Fig. 5.

For comparison, Fig. 4 also includes the methane adsorption isotherm. As it has already been mentioned in Section 2.2, methane is a smaller molecule compared to ethylene. This size difference allows that the methane molecules occupy small and large cavities. Thus, Fig. 4 shows that, for a same value of chemical potential ($\mu\approx$ -0.25), the density of methane is $\theta_{cavity}\approx$1 (one molecule per cage/cavity) while the ethylene coverage is $\theta_{cavity}\approx$1/3. In addition, in the case of methane, the maximum coverage is $\theta_{cavity}\approx$ 1.4 >1. This finding indicates that, as predicted in Ref. [71], more than one molecule can occupy the large cavities in methane hydrates, while a simple occupation of large cavities occurs in ethylene hydrates.

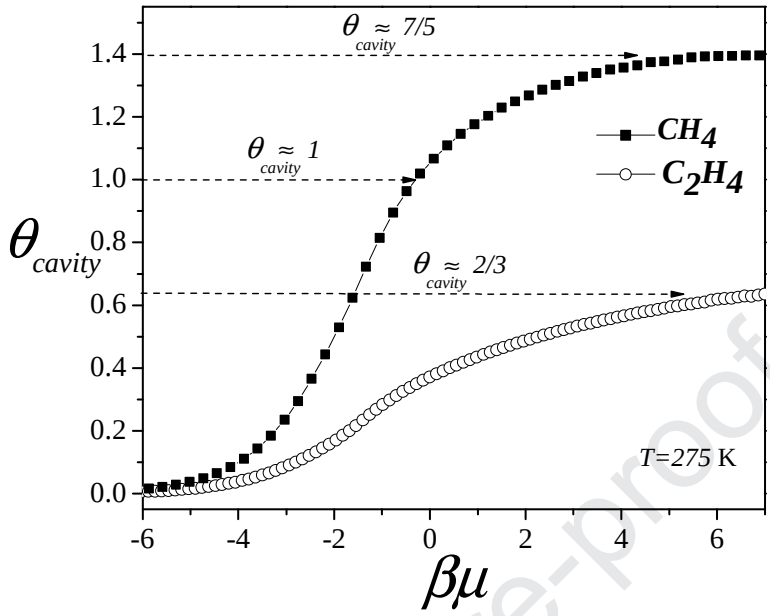

Figure 4: Adsorption isotherms for CH_4 and C_2H_4clathrate hydrates at T = 275 K.

In Section 2.3,the degree of deformation D was defined, eq.(6). The determination of D allows us to obtain information about the distortion of the 2D sI clathrate hydrate structure, due to the adsorption of ethylene in the cavities. In Fig. 5a. , the degree of deformation is plotted as a function of the coverage θ_{cavity} for ethylene hydrate clathrates and different temperature values ranging between 260K and 300K. As it has been previously stated (see discussion of Fig.4), the deformation can be associated to the relation between the size of the cavity and the guest molecule. In addition, temperature variations can cause distortions in the lattice. Hence, the degree of deformation decreases as the temperature increases. In order to interpret this behavior it is more convenient to analyze the curves in terms of the magnitude of the reduced lateral interaction ($|w_{mn}/k_BT|$). Thus, as the temperature decreases, the attractive lateral couplings become important, contributing to increase the coverage of the cavities and, accordingly, causing a distortion in the hydrate structure.

Continuing with the analysis of Fig. 5a. , the curves of $D(\theta_{cavity})$ show two minima during the filling of the cavities. The first minimum appears for values of θ_{cavity} between 0.15 and 0.20. Then, a second minimum occurs to higher values of θ_{cavity} ($0.30 < \theta_{cavity} < 0.40$). To

understand the behavior of *D*, it is useful to analyze also the free energy per site *f* as a function of θ_{cavity}. This is done in Fig. 5b. for the same cases reported in Fig. 5a. .

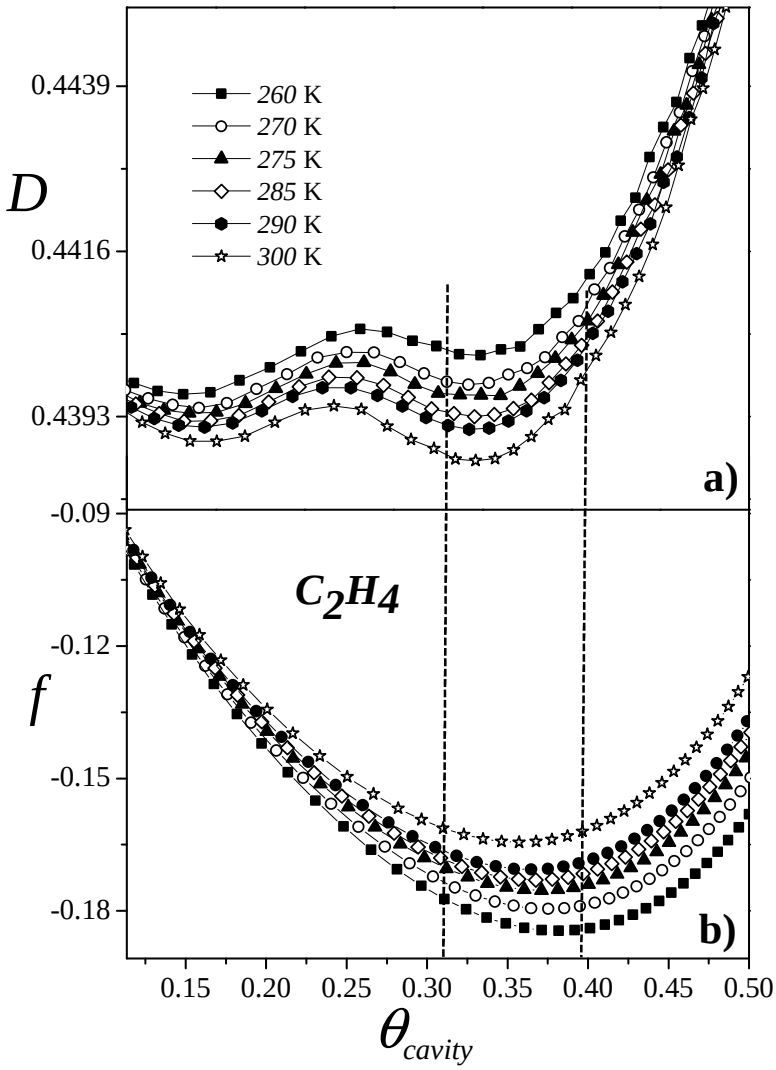

Figure 5: Degree of deformation *D* (top figure) and free energy for site *f* (bottom figure) vs. cavity coverage θ_{cavity} for ethylene hydrate clathrate at different temperatures.

By inspecting Figs. 5a. and 5b., it can be observed that the second deformation minimum coincides with the minimum values of the free energy, which means that an occupancy of $0.30 < \theta_{cavity} < 0.40$ provides higher stability to the ethylene clathrate hydrate. As the coverage θ_{cavity} is increased, the distortion increases abruptly along with the free energy,

indicating thus that the hydrate becomes unstable. In a previous work [54], we studied the behavior of the degree of deformation in the sI structure for the methane species. The obtained results showed that the minimum values of *D* and *f* agree with the location of one methane molecule per cavity. As discussed in Fig. 4, the size difference between methane and ethylene is responsible for this behavior.

With respect to the first minimum in Fig. 5a., this singularity coincides with high levels of free energy which makes the system unstable. At this coverage regime ($0.15 < \theta_{cavity} < 0.20$), a possible occupancy of small cavities could occur. We say "could" because, even though this phenomenon has already been experimentally tested [30], more investigation is needed to confirm this hypothesis. Work in this line is in progress.

A behavior qualitatively similar to that observed in Figs. 4 and 5 was obtained by using the scheme 2 for the lateral interactions (data not shown here for brevity).

According to the results presented in the in Fig.5, the stability phase diagram for ethylene clathrate hydrate is constructed considering the chemical potential $\beta\mu$ corresponding to the minimum value of *D* (and *f*). In order to compare with experimental results, it is more convenient to write the simulation data in terms of the *P*. For this purpose, a lattice-gas correction to the ideal gas approximation can be used [72, 73],

$$\mu = kT\ln(P) - kT\ln(kT/\Lambda^3) + 3kT\ln(\Delta r/\Lambda) \quad (7)$$

Where Λ is the thermal deBroglie wavelength and Δr is the separation between lattice-gas sites. In our calculations, we set $\Delta r \approx 1$nm according to the separation distance between two nearest-neighbor adsorbed ethylene molecules (see Fig. 3a., where the lattice constant is approximately 0.3 nm). The resulting stability curve is presented in Fig. 6a (solid circles). The procedure was repeated for the curves of degree of deformation and free energy for site obtained by using scheme 2. The corresponding stability curve is shown in Fig. 6a by open circles. It is important to remark that these lines are not phase coexistence lines, but lines that separate a stable from an unstable region.

In Fig. 6b., our results are compared with previous experimental and theoretical data obtained for pure ethylene clathrate hydrate [35, 71, 74, 75]: solid circles, this work (scheme 1); open circles, this work (scheme 2); squares, Ref. [35, 71]; stars, Ref. [61]; diamonds, Ref. [75]; and triangles, Ref. [74]. In both cases (scheme 1 and 2), the pressure increases monotonically with increasing temperature. However, even though the values

reported here are in the range of those previously informed in the literature, the slopes of the (P/P_0-T) curves obtained from our model are smaller than those in Refs. [35, 71, 74, 75].

The comparison between the curves calculated from schemes 1 and 2 shows that the results improve substantially when a more detailed adsorption potential is used in the simulations. Note that the slope of the (P/P_0-T) curve calculated from scheme 2 is almost 4 times bigger than the corresponding one obtained from scheme 1. Thus, the model presented here can be thought of as an initial coarse-grained model, which can serve as a starting point for addressing the complexity of dealing with clathrate hydrate phase equilibria. In this direction, our next step for further research is to develop a more refined strategy for counting the interaction energies between the adsorbed species.

As the temperature is increased above 315 K, the existence of a quadruple point Q2 (gas hydrate phase, gas phase, saturated liquid water phase and saturated guest liquid phase) for ethylene clathrate hydrate is expected [30, 32]. The point Q2 is not predictable from our model, whose starting point is a phase of frozen water forming cavities (assumed as stable) in contact with a guest gas. Consequently, the simulation results are limited only to a stable region of the hydrate due to a minimum deformation of the sI structure (minimum free energy level of the system). Last, an unstable region on account of high values from the free energy coincides with maximum values of deformation.

Summarizing, the proposed model is capable to predict some essential characteristics of the behavior of the clathrate hydrates with a not too expensive computational cost. The observed deviations with respect to the experimental points can be attributed to the limitations of a simple coarse-grained lattice-gas model. However, the understanding of simplified models, with a small number of parameters, might be a help and a guide to establish a general framework for the study of this kind of systems. The cost of introducing this kind of models is the lack of some experimental features presented by real systems.

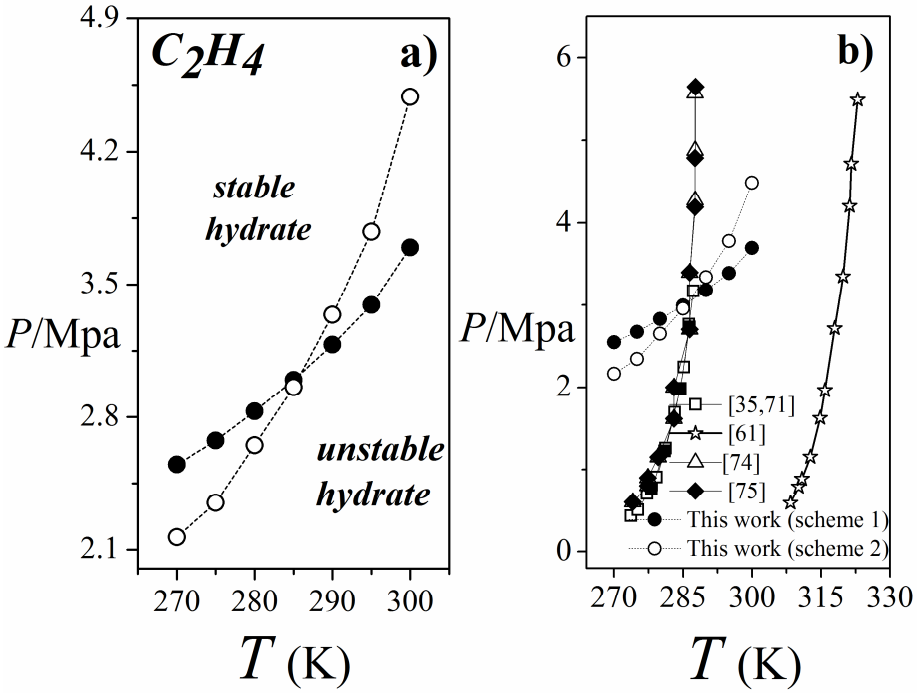

Figure 6: a) Phase diagrams *P* (Mpa) vs *T* for ethylene hydrate clathrate. Solid and open circles represent simulation data obtained by using schemes 1 and 2, respectively. Up to the stability line the hydrate is in a stable stage. While, under the stability line the hydrate is unstable. The stability line is not a line of coexistence of phases. However, this line is in a qualitative agreement with phase diagrams of part b). **b)** Experimental and theoretical phase diagrams *P* vs *T* for ethylene hydrate clathrate obtained from :squares, –F. Ma et al. [35] and L. E. Snell et al. [71]; stars, M. Lasichet al [61]; diamonds, K. Tumba, et al. [75]; and triangles, M. Lasich [74].

4. Conclusions

It is clear that a complete analysis of the stability and degree of deformation of gas hydrates in the presence of guest species is a quite difficult subject because of the complexity of the involved systems. For this reason, the understanding of simple models with increasing complexity might be a help and a guide to establish a general framework for the study of this kind of systems. In this context, the present work tries to contribute to the comprehension of some essential characteristics of sI clathrate hydrates of ethylene by means of a very simple model. For this purpose, Monte Carlo simulations in the framework of a 2D lattice gas-model have been used. The adsorption process has been monitored by following the adsorption isotherm (coverage of the cavities θ_{cavity} as a function of the

chemical potential (μ), the degree of deformation of the sI structure, and the free energy of the adsorbed phase.

Two levels of approximation were considered for the lateral interactions between the adsorbed molecules: scheme 1, where each ethylene molecule interacts with the surrounding species through its four ends; and scheme 2, where the interactions corresponding to the internal units of the ethylene molecule are also considered. In both cases, the obtained results for the adsorption isotherm indicate that ethylene molecules adsorb in the largest cavities, generating a distortion in the lattice and preventing the occupancy of the small cavities. The maximum coverage reached θ_{cavity} = 2/3 (one molecule per each large cavity) contrasts with the corresponding value of $\theta_{cavity}\approx$ 1.4 for methane (more than one molecule per cavity). This behavior can be understood from the size difference between methane and ethylene.

The degree of deformation of the lattice (*D*) and the free energy per site of the adsorbed phase (*f*) were calculated as a function of the cavity density. The curve of *D* shows two minima. The first minimum coincides with high levels of free energy which makes the system unstable. At this coverage regime, a possible occupancy of small cavities could occur. As mentioned in previous section, more investigation is needed to confirm or discard this conjecture.

In addition, the behavior of *D* and *f* relates to the stability of sI structure. In fact, the second deformation minimum, which coincides with the minimum values of the free energy, allows to determine the stability region to the ethylene clathrate hydrate. The obtained results indicate that the most stable condition of the system occurs for values of the cavity density ranging between 0.35 and 0.4. In the case of methane hydrates, the most stable state was found at coverage close to one (one methane molecule per cavity) [54].

Finally, the (P/P_0-T) phase diagram was calculated from the values of the chemical potential at the minimum deformation. The resulting curve, which separates a stable region from an unstable region, was compared with previous experimental and theoretical data [35, 71, 74, 75]. Even though an increasing (P/P_0-T) behavior was obtained in the present work, the slope of the curve differs from that in previous studies. Our work also shows that the results of the model improve with a more refined counting of the lateral interactions. Thus, as an illustrative example, the slope of the (P/P_0-T) curve calculated from scheme 2

is almost 4 times bigger than the corresponding one obtained from scheme 1. These findings (i) encourage the development of more sophisticated counting procedures for determining the adsorption force field; and (ii) suggest that the model introduced here may be a good starting point for studying the rich problem of clathrate hydrate phase equilibria. Our approach may not be as accurate as other techniques such as molecular dynamics simulations, but it is elegant, computationally inexpensive and, with slight modifications, could be applied to other related areas such as adsorption in zeolites and metal-organic frameworks. In this line, future research will be directed (1) to estimating more precisely the couplings between adsorbed units, considering their chemical nature and spatial distribution; and (2) to extending the lattice-gas simulation model to three-dimensional systems.

Acknowledgments

This work was supported in part by CONICET (Argentina) under project number PIP 112-201701-00673CO; Universidad Nacional de San Luis (Argentina) under project No. 03-0816; and the National Agency of Scientific and Technological Promotion (Argentina) under project PICT-2013-1678.

References

[1] E. D. Sloan, Fundamental principles and applications of gas hydrates, Nature 426 (2003) 353–359, https://doi.org/10.1038/nature02135.

[2] E. D. Sloan, C. A. Khoh, Clathrate Hydrates of Natural Gases, CRC Press, USA, 2007.

[3] J. L. Atwood, J. E. D. Davies, D.D. McNicol, Inclusion Compounds, Academic Press, London, 1984.

[4] G. A. Jeffrey, R. K. McMullan, The clathrate hydrates, Prog. Inorg. Chem. 8 (1967) 43–108, https://doi.org/10.1002/9780470166093.ch2.

[5] T. S. Collett, Energy resource potential of natural gas hydrates, AAPG Bull. 86 (2002) 1971–1992, https://doi.org/10.1306/61EEDDD2-173E-11D7-8645000102C1865D.

[6] M. R. Walsh, S.H. Hancock, S. Wilson, S. L. Patil, G. J. Moridis, R. Boswell, T. S. Collett, C.A. Koh, E. D. Sloan, Preliminary report on the commercial viability of gas

production from natural gas hydrates, Energy Economics 31 (2009) 815–823, https://doi.org/10.1016/j.eneco.2009.03.006.

[7] G. J. Moridis, T. S. Collett, R. Boswell, M. Kurihara, M. T. Reagan, C. Koh, E. D. Sloan, Towards production from gas hydrates: current status, assessment of resources, and simulation based evaluation of technology and potential, SPE Reservoir Eval. Eng. 12 (2009) 745–771, http://pubs.er.usgs.gov/publication/70037371ER.

[8] K. A. Kvenvolden, A review of the geochemistry of methane in natural gas hydrate, Org. Geochem. 23 (1995) 997–1008, https://doi.org/10.1016/0146-6380 (96)00002-2.

[9] J. B. Klauda, S.I. Sandler, Global distribution of methane hydrate in ocean sediment, Energy Fuels 19 (2005) 459–470, https://doi.org/10.1021/ef049798o.

[10] E. G. Hammerschmidt, Formation of gas hydrates in natural gas transmission lines, Ind. Eng. Chem. 26 (1934) 851–855, https://doi.org/10.1021/ie50296a010.

[11] I. Chatti, A. Delahaye, L. Fournaison, J. P. Petitet, Benefits and drawbacks of clathrate hydrates: a review of their areas of interest, Energy Convers. Manage. 46 (2005) 1333–1343, https://doi.org/10.1016/j.enconman.2004.06.032.

[12] X. Wang, M. Dennis, L. Hou, Clathrate hydrate technology for cold storage in air conditioning systems, Renew. Sustain. Energy Rev. 36 (2014) 34–51, https://doi.org/10.1016/j.rser.2014.04.032.

[13] J. Zhao, Y. Zhao, W. Liang, CH_4 Separation from Coal Bed Methane by Hydrate in the SDS and THF Solution. *Journal of Chemistry* 2016 (2016) 1-6, http://dx.doi.org/10.1155/2016/9575736.

[14] A. Eslamimanesh, A. H. Mohammadi, D. Richon, P. Naidoo, D. Ramjugernath, Application of gas hydrate formation in separation processes: a review of experimental studies, J. Chem. Thermodynam. 46 (2012) 62–71, https://doi.org/10.1016/j.jct.2011.10.006.

[15] P. Babu, P. Linga, R. Kumar, P. Englezos, A review of the hydrate based gas separation (HBGS) process for carbon dioxide pre-combustion capture, Energy 85 (2015) 261–279, https://doi.org/10.1016/j.energy.2015.03.103.

[16] C. Xu, X. Li, Research progress of hydrate–based CO_2 separation and capture from gas mixtures, RSC Adv. 4 (2014) 492–504, http://dx.doi.org/10.1039/C4RA00611A.

[17] P. Naeiji, M. Mottahedin, F. Varaminian, Separation of methane–ethane gas mixtures via gas hydrate formation, Sep. Purif. Technol. 123 (2014) 139–144, https://doi.org/10.1016/j.seppur.2013.12.028.

[18] X. Zhang, H. Liu, C. Sun, P. Xiao, B. Liu, L. Yang, C. Zhan, X. Wang, N. Li, G. Chen, Effect of water content on separation of CO_2/CH_4 with active carbon by adsorption - hydration hybrid method, Sep. Purif. Technol. 130 (2014) 132–140, https://doi.org/10.1016/j.seppur.2014.04.028.

[19] J. H. Cha, Y. Seol, Increasing gas hydrate formation temperature for desalination of high salinity produced water with secondary guests, ACS Sustain. Chem. Eng. 1 (2013) 1218–1224, https://doi.org/10.1021/sc400160u.

[20] S. Han, J. Y. Shin, Y.W. Rhee, S. P. Kang, Enhanced efficiency of salt removal from brine for cyclopentane hydrates by washing, centrifuging, and sweating, Desalination 354 (2014) 17–22, https://doi.org/10.1016/j.desal.2014.09.023.

[21] Y. A. Purwanto, S. Oshita, Y. Seo, Y. Kawagoe, Concentration of liquid foods by the use of gas hydrate, J. Food Eng. 47 (2001) 133–138, https://doi.org/10.1016/S0260-8774(00)00109-6.

[22] S. Li, Y. Shen, D. Liu, L. Fan, Z. Tan, Concentrating orange juice through CO_2 clathrate hydrate technology, Chem. Eng. Res. Des. 93 (2015) 773–778, https://doi.org/10.1016/j.cherd.2014.07.020.

[23] S. Li, F. Qi, K. Dua, Y. Shen, D. Liu, L. Fan, An energy-efficient juice concentration technology by ethylene hydrate formation Sep. Purif. Technol. 173 (2017) 80–85, https://doi.org/10.1016/j.seppur.2016.09.021.

[24] H. Liu, L. Mu, B. Liu, X. Zhang, J. Wang, B. Wang, C. Sun, L. Yang, H. Wang, P. Xiao, G. Chen. Experimental studies of the separation of C_2 compounds from CH_4 + C_2H_4 + C_2H_6 + N_2 gas mixtures by absorption-hydration hybrid method. Ind. Eng. Chem. Res. 52(2013) 2707–2713, https://doi.org/10.1021/ie3028526.

[25] H. Liu, L. Mu, B. Wang, B. Liu, J. Wang, X.X. Zhang, C. Y. Sun, J. Chen, M. L. Jia, G. J. Chen. Separation of ethylene from refinery dry gas via forming hydrate in w/o dispersion system. Sep. Purif. Technol. 116 (2013) 342–350, https://doi.org/10.1016/j.seppur.2013.06.008.

[26] Y. Pan, H. Liu, Z. Li, B. Liu, Q. Ma, G. Chen, C. Sun, L. Yang, X. Gao, Ethylene Separation via hydrate formation in w/o emulsions, Energies 8 (2015) 4871-4881, https://doi.org/10.3390/en8064871.

[27] J. Liu, H. Pan, Y. Zhou, L. Zhou, Formation pressure of ethylene hydrates in carbon pores at near-critical temperature, J. Chem. Eng. Data 57 (2012) 2549– 2552, https://doi.org/10.1021/je300614z.

[28] Y. Wanga, J. Zhanga, X. Guob, B. Chena, Q. Suna, A. Liub, C. Suna, G. Chena, L. Yanga, Experiments and modeling for recovery of hydrogen and ethylene from fluid catalytic cracking (FCC) dry gas utilizing hydrate formation, Fuel 209 (2017) 473-489, https://doi.org/10.1016/j.fuel.2017.07.108.

[29] G. A. M. Diepen, F. E. C. Scheffer, The ethene-water system. Recueil des Travaux Chimiques des Pays-Bas. 69 (2010) 593 – 603, https://doi.org/10.1002/recl.19500690513.

[30] T. Sugahara, K. Morita, K. Ohgaki, Stability boundaries and small hydrate-cage occupancy of ethylene hydrate system, Chemical Engineering Science, 55 (2000) 6015-6020, https://doi.org/10.1016/S0009-2509(00)00226-8.

[31] A. H. Mohammadi, D. Richon, Clathrate hydrate phase equilibria for carbonyl sulfide, hydrogen sulfide, ethylene, or propane + water system below water freezing point, Chem. Eng. Commun. 200 (2013) 1635–1644, https://doi.org/10.1080/00986445.2012.757550.

[32] K. Tumba, H. Hashemi, P. Naidoo, A. H. Mohammadi, D. Ramjugernath, Dissociation data and thermodynamic modeling of clathrate hydrates of ethene, ethyne, and propene, J. Chem. Eng. Data 58 (2013) 3259–3264, https://doi.org/10.1021/je400727q.

[33] M. Manteghian, S. M. M. Safavi, A. Mohammadi, The equilibrium conditions, hydrate formation and dissociation rate and storage capacity of ethylene hydrate in presence of 1,4-dioxane, Chem. Eng. J. 217 (2013) 379–384, https://doi.org/10.1016/j.cej.2012.12.014.

[34] Y. Wei, Y. Sun, W. Su, J. Liu, Influence of pore size on ethylene hydrate formation in carbon materials, Adsorpt. Sci. Technol. 32 (2014) 717–724, https://doi.org/10.1260/0263-6174.32.9.717.

[35] C. –F. Ma, G. –J. Chen, F. Wang, C. –Y. Sun, T. -M. Guo, Hydrate formation of (CH_4 + C_2H_4) and (CH_4 + C_3H_6) gas mixtures. Fluid Phase Equilibria 191 (2001) 41–47, https://doi.org/10.1016/S0378-3812(01)00610-0.

[36] S. Shahnazar, N. Hasan, Gas hydrate formation condition: Review on experimental and modeling approaches, Fluid Phase Equilibria 379 (2014) 72-85, https://doi.org/10.1016/j.fluid.2014.07.012.

[37] J. H. van der Waals, J. C. Platteeuw, Clathrate solutions, Adv. Chem. Phys. 2 (1958) 1 -57, https://doi.org/10.1002/9780470143483.ch1.

[38] W. R. Parrish, J.M. Prausnitz, Dissociation pressures of gas hydrates formed for by gas mixtures, Ind. Eng. Chem. Process Des. Dev. 11 (1972) 26–35, https://doi.org/10.1021/i260041a006.

[39] H. Tanaka, The thermodynamic stability of clathrate hydrate. III. Accommodation of nonspherical propane and ethane molecules, J. Chem. Phys. 101 (1994) 10833–10842, https://doi.org/10.1063/1.467832.

[40] R. E. Westacott, M. P. Rodger, Full-coordinate free-energy minimisation for complex molecular crystals: type I hydrates, Chem. Phys. Lett. 262 (1996) 47–51, https://doi.org/10.1016/0009-2614(96)01042-1.

[41] H. Tanaka, T. Nakatsuka, K. Koga, On the thermodynamic stability of clathrate hydrates IV: double occupancy of cages, J. Chem. Phys. 121 (2004) 5488–5493.

[42] A. A. Chialvo, M. Houssa, P.T. Cummings, Molecular dynamics study of the structure and thermophysical properties of model sI clathrate hydrates, J. Phys. Chem. B 106 (2002) 442–451, https://doi.org/10.1021/jp012735b.

[43] P. M. Rodger, Lattice relaxation in type I gas hydrates, AIChE J. 37 (1991) 1511–1516, https://doi.org/10.1002/aic.690371008.

[44] S. R. Zele, S. -Y. Lee, G.D. Holder, A theory of lattice distortion in gas hydrates, J. Phys. Chem. B 103 (1999) 10250–10257, https://doi.org/10.1021/jp9917704.

[45] S. J. Wierzchowski, P. A. Monson, Calculation of free energies and chemical potentials for gas hydrates using Monte Carlo simulations, J. Phys. Chem. B 111 (2007) 7274–7282, https://doi.org/10.1021/jp068325a.

[46] V. Vladimir Sizov, M. Elena Piotrovskaya, Computer simulation of methane hydrate cage occupancy, J. Phys. Chem. B 111 (2007) 2886–2890, https://doi.org/10.1021/jp0658905.

[47] N. I. Papadimitriou, I. N. Tsimpanogiannis, A. Th Papaioannou, A. K. Stubos, Evaluation of the hydrogen-storage capacity of pure H_2 and binary H_2-THF hydrates with

Monte Carlo simulations, J. Phys. Chem. C 112 (2008) 10294–10302, https://doi.org/10.1021/jp074706s.

[48] N. I. Papadimitriou, I. N. Tsimpanogiannis, A. K. Stubos, Monte Carlo simulations of methane hydrates, Proceedings of the 7th International Conference on GasVHydrates (ICGH 2011), Edinburgh, Scotland, United Kingdom, 2011, https://www.pet.hw.ac.uk/icgh7/papers/icgh2011Final00560.pdf

[49] H. Pimpalgaonkar, S. K. Veesam, S. N. Punnathanam, Theory of gas hydrates: effect of the approximation of rigid water lattice, J. Phys. Chem. B 115 (2011) 10018–10026, https://doi.org/10.1021/jp204129t.

[50] N. I. Papadimitriou, I. N. Tsimpanogiannis, A. K. Stubos, A. Martín, L. J. Rovetto, L. J. Florusse, C. J. Peters, Experimental and computational investigation of the Sii binary He-THF hydrate, J. Phys. Chem. B 115 (2011) 1411–1415, https://doi.org/10.1021/jp105451m.

[51] A. Martín, C. J. Peters, New thermodynamic model of equilibrium states of gas hydrates considering lattice distortion, J. Phys. Chem. C 113 (2009) 422–430, https://doi.org/10.1021/jp8074546.

[52] H. J. C. Berendsen, J. R. Grigera, T. P. Straatsma, The missing term in effective pair potentials, J. Phys. Chem. 91 (1987) 6269–6271, https://doi.org/10.1021/j100308a038.

[53] W. L. Jorgensen, J. D. Madura, C. J. Swenson, Optimized intermolecular potential functions for liquid hydrocarbons, J. Am. Chem. Soc. 106 (1984) 6638–6646, https://doi.org/10.1021/ja00334a030.

[54] P. Longone , A. Martín, A. J. Ramirez-Pastor, Stability and cell distortion of sI clathrate hydrates of methane and carbon dioxide: A 2D lattice-gas model study, Fluid Phase Equilibria, 402 (2015) 30–37, https://doi.org/10.1016/j.fluid.2015.05.035.

[55] Chaplin, M., Water structure and science, [on-line]. This work is licensed under a Creative Commons Attribution-Noncommercial-No Derivative Works 2.0 UK: England & Wales License. G. Crane, Editor-in-Chief. <http://www1. lsbu.ac.uk/water/clathrat2.html#si>, 2003.

[56] J. E. González, A. J. Ramirez-Pastor, V. D. Pereyra, Adsorption of dimer moleculeson triangular and honeycomb lattices, Langmuir 17 (2001) 6974–6980, https://doi.org/10.1021/la010465i.

[57] A. J. Ramirez-Pastor, M. S. Nazzarro, J. L. Riccardo, G. Zgrablich, Dimer physisorption on heterogeneous substrates, Surf. Sci. 341 (1995) 249–261, https://doi.org/10.1016/0039-6028(95)00665-6.

[58] M. C. Giménez, A. J. Ramirez-Pastor, E. P. M. Leiva, Monte Carlo simulation of metal deposition on foreign substrates, Surf. Sci. 600 (2006) 4741–4751, https://doi.org/10.1016/j.susc.2006.07.050.

[59] R.T. Morrison, R.N. Boyd, *Organic Chemistry*, Prentice-Hall International, New Jersey, 1992.

[60] R. K. McMullan , G. A. Jeffrey, Polyhedral Clathrate Hydrates. IX. Structure of Ethylene Oxide Hydrate, J. Chem. Phys. 42 (1965) 2725-2732 , https://doi.org/10.1063/1.1703228.

[61] M. Lasich, D. Ramjugernath, Clathrate hydrates modelled with classical density functional theory coupled with a simple lattice gas and van der Waals-Platteeuw theory, Philosophical Magazine, 96 (2016) 2853-2867, https://doi.org/10.1080/14786435.2016.1217093.

[62] W.M. Deaton, E.M. Frost Jr., Gas Hydrates and their Relation to the Operation of Natural Gas Pipeline, U.S. Bureau of Mines Monograph, New York, 8, 1946.

[63] D.R. Marshall, S. Saito, R. Kobayashi, Carbon monoxide clathrate hydrates: Equilibrium data and thermodynamic modeling AIChE J. 10 (1964) 202- 205, https:// doi.org/10.1002/aic.690100214.

[64] A.H. Mohammadi, R. Anderson, B. Tohidi, Carbon monoxide clathrate hydrates: Equilibrium data and thermodynamic modeling, AIChE J. 51 (2005) 2825–2833. https://doi.org/10.1002/aic.10526.

[65] H. A. Lorentz, Ueber die Anwendung des Satzes vom Virial in der kinetischen Theorie der Gase, Ann. Phys. 12 (1881) 127-136, https://doi.org/10.1002/andp.18812480110.

[66] H. A. Lorentz, Nachtrag zu der Abhandlung: Ueber die Anwendung des Satzes vom Virial in der kinetischen Theorie der Gase, Ann. Phys. 12 (1881) 660-661, https://doi.org/10.1002/andp.18812480414

[67] D. Berthelot, Sur le Mélange des Gaz, Compt. Rend. Acad. Sci. 126 (1898) 1703–1706; 126 (1898) 1857–1858.

[68] N. Metropolis, A. W. Rosenbluth, M. N. Rosenbluth, A. H. Teller, E. Teller, Equation of state calculations by fast computing machines, J. Chem. Phys. 21 (1953) 1087–1092, https://doi.org/10.1063/1.1699114.

[69] K. Binder, Static and dynamic critical phenomena of the two-dimensional q state Potts model, J. Stat. Phys. 24 (1981) 69–86, https://doi.org/10.1007/BF01007636.

[70] E. D. Sloan, Clathrate hydrates of natural gases, Marcel Dekker, New York, 1990.

[71] L. E. Snell, F. D. Otto, D. B. Robinson, AIChE J. 7 (1961) 482–485, https://doi.org/10.1002/aic.690070328.

[72] T. L. Hill, *An Introduction to Statistical Thermodynamics*, Addison-Wesley, Reading, MA, 1960.

[73] A. Valencia, M. Brinkmann, R. Lipowsky, Liquid bridges in chemically structured slit pores, Langmuir 17 (2001) 3390–3399, https://doi.org/10.1021/la001749q.

[74] M. Lasich, An improved description of clathrate hydrates using classical density functional theory coupled with a simple lattice gas and van derWaals- Platteeuw theory, Fluid Phase Equilibria 456 (2018) 131-139, https://doi.org/10.1016/j.fluid.2017.10.010.

[75] K. Tumba, P. Naidoo, A.H. Mohammadi, D. Richon, D. Ramjugernath, Dissociation Data and Thermodynamic Modeling of Clathrate Hydrates of Ethene, Ethyne, and Propene, J. Chem. Eng. Data 58 (2013). 3259-3264, https://doi.org/10.1021/je400727q.

Declaration of interests

☒ The authors declare that they have no known competing financial interests or personal relationships that could have appeared to influence the work reported in this paper.

☐The authors declare the following financial interests/personal relationships which may be considered as potential competing interests: